PHYSICAL REVIEW C VOLUME 24, NUMBER 5 NOVEMBER 1981

Momentum transfer in the fragmentation of Cu by relativistic heavy ions and protons

J. B. Cumming, P. E. Haustein, and H.-C. Hseuh
Chemistry Department, Brookhaven National Laboratory, Upton, New York 11973
(Received 22 June 1981)

Mean kinetic properties of selected products from the fragmentation of Cu by ^{1}H, ^{4}He, and ^{12}C ions over energies ranging from 0.18 to 28 GeV/nucleon have been determined by the thick-target, thick-catcher technique. Momentum transfer, as inferred from F/B ratios, is observed to occur most efficiently for the lower velocity projectiles. Recoil properties of the target fragments, analyzed using the two step velocity vector model, vary strongly with product mass. Rapidity (or some other velocity related parameter) is the dominant projectile variable which governs momentum transfers to fragments from Cu. This and previous observations of the importance of kinetic energy in determining fragment yields are shown to be consistent with a simple kinematical model for the fragmentation process. Major deviations from such simple behavior are observed for high-energy heavy ions incident on heavy element targets.

[NUCLEAR REACTIONS Cu fragmentation by ^{1}H, ^{4}He, and ^{12}C, $T/A = 0.18$ to 28 GeV/nucleon, thick target, thick catchers; measured *FW*, *BW*, and *PW* for six selected products: ^{24}Na to ^{58}Co, deduced mean kinetic properties, natural targets, Ge(Li) detectors.]

I. INTRODUCTION

The decade since the first successful acceleration of heavy ions to relativistic energies[1,2] has seen numerous investigations of their interactions with complex nuclei.[3] Many features of such reactions can be understood in terms of a two-step mechanism[4] in which the excitation and deexcitation stages are separated temporally. In the first or abrasion step, as treated by the fireball,[5] firestreak,[6] or rows-on-rows[7] models, only those nucleons in the region of overlap ("participants") take part in the interaction between the target and passing projectile. Spectator parts of both—"prefragments"—remain relatively undisturbed in their state of motion (or rest) but may be excited and decay, e.g., by particle emission, to the observed products in the subsequent ablation step. These models emphasize the geometrical aspects of the collisions, in particular the role of the impact parameter. They suggest a division of products into three groups on the basis of fragment velocities. Projectile fragments appear in a distribution near the projectile velocity; those from the target are found nearly at rest in the laboratory system, with nucleons and small fragments from the highly excited intersecting region (fireball) appearing at intermediate values. Central or near central collisions appear as violent events[8] in which both target and projectile disintegrate into a high multiplicity shower of nucleons and small fragments.[9] The present work focuses on the more probable, peripheral events which lead to massive target (or projectile) residues, the role of target or projectile being determined by choice of the reference frame.

In addition to the above geometrical picture, two hypotheses originally applied to energetic hadron-hadron interactions have proven to be a useful framework for describing nucleus-nucleus interactions.[10] The hypothesis of *limiting fragmentation* predicts that both the cross section and energy spectra of a fragment in its proper frame (either projectile or target) should become independent of bombarding energy at sufficiently high energies. The second, *factorization,* asserts that these fragment properties can be written as a product of target and beam factors. The distribution of target fragments then will be independent of the nature of the beam except for a constant term (the ratio of projectile factors) and vice versa for projectile fragments.

Evidence for the general validity of these notions

 ©1981 The American Physical Society

comes from studies[11–13] of the fragmentation of ^{12}C, ^{16}O, and ^{56}Fe projectiles on a variety of targets and from data on the fragmentation of Cu,[14–16] Ag,[17,18] Ta,[19,20] Au,[20–22] Pb,[21] and U (Ref. 23) targets by projectiles ranging up to ^{40}Ar. These experiments indicate that projectile kinetic energy is the important parameter in determining fragment yield distributions. The onset of the limiting fragmentation region (as measured by the slope of the mass yield curve) has been inferred to occur at ~ 3 GeV kinetic energy for the Cu system.[16] However, other data show that appreciable differences persist to higher energies for the heavier targets. When U is irradiated with 25-GeV ^{12}C ions, the mass yield curve shows[23] a peak at $160 \lesssim A \lesssim 190$ which has no counterpart for other projectiles.

More detailed information on target fragmentation processes can be gained through measurements of fragment kinematics. In particular, the thick-target, thick-catcher technique can give information on $\beta_{||}$, the velocity (in units of c) of the excited prefragments after the abrasion step and on V, the additional component of velocity imparted by ablation. Experiments[24] on the 25-GeV ^{12}C and 28-GeV ^{1}H fragmentation of copper showed identical values of V for the several products studied (from $A=58$ to $A=24$), but enhanced (23%) values of $\beta_{||}$ for the heavy projectile. Comparing these data with those for the proton and alpha particle spallation[25] led to the conclusion that the limiting fragmentation region had not yet been reached for 25-GeV ^{12}C and further suggested that momentum transfers in the abrasion step depended on projectile rapidity ($Y=\tanh^{-1}\beta$) or some other velocity related variable, rather than its kinetic energy or momentum. This is in contrast with results from similar studies[26] of Au targets where momentum transfers to prefragments were found to be the same for 25-GeV ^{12}C and 28-GeV ^{1}H projectiles, suggesting, as was concluded from the cross section studies, that kinetic energy is the determining parameter. Recent results for 4.8-GeV ^{12}C and 8.0-GeV ^{20}Ne ions impinging on Ta and Au targets[22,27] show that momentum transfers are substantially greater than those observed with 25-GeV ^{12}C ions or 28-GeV protons and apparently greater than those which would be observed at any proton energy. The momentum transfers in the case of Au were found[22] to be essentially the same for 4.8-GeV ^{12}C and 7.6-GeV ^{20}Ne projectiles.

The present experiment extends the previous studies of the kinematics of fragmentation processes in Cu targets to lower energies (4.8-GeV ^{12}C and 0.8-GeV ^{1}H) and adds results for a projectile of intermediate mass, ^{4}He. A preliminary report on some of the new results has been given.[28]

II. EXPERIMENTAL

The experimental techniques used in the present study are essentially those described previously.[24,28] Thick-target, thick-catcher stacks were irradiated with a variety of light- and heavy-ion beams at various accelerators. Table I summarizes this; it is ordered by projectile kinetic energy per nucleon (T/A) and lists the approximate fluence of particles. Target stacks consisted of 109-mg/cm^2 Cu foils with 18-mg/cm^2 Mylar catcher foils on the upstream and downstream sides. An additional Mylar foil on the upstream side served as a blank, and the four foils were vacuum encapsulated between pieces of 12-mg/cm^2 heat-sealable Mylar. In five of the irradiations, two such stacks, separated by 10 cm, were exposed simultaneously. The beam was incident normally on the first, but entered the second at a 20° angle to its surface. Only the configuration of normal incidence was used in the ex-

TABLE I. Proton and heavy-ion beams used in the thick-target, thick-catcher studies of Cu target fragmentation.

Ion	Kinetic energy (T) (GeV)	T/A (GeV/nucleon)	Rapidity	Fluence	Lab
^{4}He	0.72	0.18	0.612	2×10^{15}	SREL
^{12}C	4.8	0.40	0.896	1×10^{14}	LBL
^{1}H	0.81	0.81	1.241	3×10^{14}	BNL
^{4}He	4.0	1.0	1.358	5×10^{14}	LBL
^{12}C	25.2[a]	2.1	1.849	8×10^{12}	LBL
^{1}H	28.0[a]	28.0	4.129	1×10^{14}	BNL

[a]Results of these irradiations have been analyzed in part in Ref. 24.

periment with 0.81-GeV protons.

After an irradiation, the activities of ^{24}Na, ^{28}Mg, ^{44}Sc^{m}, ^{48}V, ^{52}Mn, and ^{58}Co were determined in the various foils from the counting rates of the more intense γ rays in each decay as measured with shielded Ge(Li) detectors.

Basic results from each experiment are the three quantities *FW*, *BW*, and *PW* which are listed in Table II. *F* and *B* are the fractions of the activity produced in the target of thickness *W* mg/cm^2 which were observed in the downstream and upstream catchers, respectively, of the first stack. The quantity *P* is the mean of the fractions observed in the more-forward and more-backward catchers of the inclined stack. Blanks due to activation of impurities in the Mylar foils were negligible for all isotopes except ^{24}Na. Even in that case, corrections were generally the order of a few percent. In the worst case, that for 0.72-GeV ^{4}He, the tabulated value of *BW* was reduced by 13% from the raw value.

Some systematic trends are apparent in these experimental data without more detailed analysis: First, for a given projectile and energy, *FW*, *BW*, and *PW* decrease smoothly from the light products, ^{24}Na and ^{28}Mg, to the heavier, near-target products such as ^{58}Co. Second, the entries in Table II for a particular isotope appear to vary smoothly with some function of the projectile's velocity. The rows in Table II were ordered according to projectile *T/A* to emphasize this effect. The general fall of *FW*, rise of *BW*, and relative constancy of *PW* with increasing *T/A* are similar to dependencies observed for proton induced reactions.[29]

III. RESULTS AND DISCUSSION

It is informative to analyze the present results in terms of a two-step model[30–32] for the interaction, a model commonly referred to as cascade plus evaporation in the case of incident nucleons, or what

TABLE II. Recoil properties of selected products from the interaction of energetic protons and heavy ions with copper.[a]

Projectile, GeV/nucleon	^{24}Na	^{28}Mg	^{44}Sc^{m}	^{48}V	^{52}Mn	^{58}Co
			FW (mg/cm^2)			
^{4}He, 0.18	1.844(70)	1.99(39)	1.084(15)	0.917(16)	0.749(07)	0.330(13)
^{12}C, 0.40	1.770(17)	1.79(08)	0.851(08)	0.673(04)	0.530(05)	0.232(03)
^{1}H, 0.81	1.378(83)	1.38(08)	0.617(08)	0.500(03)	0.409(07)	0.191(03)
^{4}He, 1.0	1.302(37)	1.36(17)	0.631(10)	0.495(21)	0.409(10)	0.183(12)
^{12}C, 2.1 (Ref. 24)	0.998(24)	1.08(06)	0.526(08)	0.431(10)	0.356(23)	0.171(12)
^{1}H, 28. (Ref. 24)	0.957(32)	0.96(03)	0.460(05)	0.364(04)	0.307(04)	0.136(03)
			BW (mg/cm^2)			
^{4}He, 0.18	0.179(55)	0.33(19)	0.037(02)	0.040(06)	0.021(02)	0.022(05)
^{12}C, 0.40	0.198(05)	0.21(02)	0.066(01)	0.055(02)	0.046(01)	0.036(02)
^{1}H, 0.81	0.356(34)	0.36(03)	0.099(02)	0.083(02)	0.068(01)	0.042(01)
^{4}He, 1.0	0.300(19)	0.48(10)	0.130(05)	0.115(15)	0.101(07)	0.062(10)
^{12}C, 2.1 (Ref. 24)	0.376(13)	0.40(04)	0.156(05)	0.134(07)	0.111(06)	0.065(06)
^{1}H, 28. (Ref. 24)	0.430(17)	0.44(02)	0.166(03)	0.133(02)	0.109(02)	0.058(02)
			PW (mg/cm^2)			
^{4}He, 0.18	0.810(30)	0.92(15)	0.390(03)	0.313(06)	0.261(02)	0.133(03)
^{12}C, 0.40	0.851(08)	0.87(03)	0.365(04)	0.299(03)	0.244(03)	0.121(02)
^{1}H, 0.81						
^{4}He, 1.0	0.727(13)	0.80(04)	0.333(05)	0.278(06)	0.226(03)	0.120(05)
^{12}C, 2.1	0.718(08)	0.66(03)	0.326(05)	0.284(04)	0.232(03)	0.127(04)
^{1}H, 28.	0.654(04)	0.61(02)	0.291(02)	0.238(02)	0.198(01)	0.099(02)

[a]The error on each tabulated value is shown in parentheses, e.g., 1.844(70) is to read as 1.840 ± 0.070.

TABLE III. Summary of minimum b/a values consistent with the experimental data.[a]

Projectile Isotope	0.72 GeV ^{4}He	4.8 GeV ^{12}C	4.0 GeV ^{4}He	25 GeV ^{12}C	28 GeV ^{1}H
^{24}Na	−0.18±0.36	−0.37±0.04	−0.11±0.13	−0.37±0.07	+0.08±0.16
^{28}Mg	+0.27±1.51	−0.33±0.18	+0.30±0.64	+0.25±0.37	+0.52±0.23
^{44}Sc^m	−0.12±0.08	−0.20±0.06	+0.01±0.10	−0.15±0.08	+0.06±0.05
^{48}V	+0.43±0.24	−0.29±0.05	−0.09±0.23	−0.30±0.09	−0.06±0.05
^{52}Mn	−0.10±0.09	−0.36±0.05	+0.06±0.14	−0.26±0.18	−0.05±0.05
^{58}Co	−0.09±0.28	−0.28±0.08	−0.18±0.30	−0.43±0.18	−0.24±0.10
Mean	−0.08±0.06	−0.32±0.02	−0.02±0.06	−0.28±0.04	−0.02±0.03

[a]Essentially identical values of b/a are calculated from the conventional equations (Ref. 33) when $v_\perp=0$. However, error estimates are not readily obtainable.

is equivalent, abrasion-ablation if the projectile is a heavy ion. Such a treatment assumes that the velocity distribution of a product can be resolved into two components, a $\vec{v}$ resulting from the initial projectile-target interaction, and a $\vec{V}$ arising from the subsequent deexcitation of the excited prefragment to yield the observed product. The vector $\vec{v}$ may have components $v_{||}$ and $v_\perp$ measured with respect to the beam direction, and $\vec{V}$ may have an anisotropic angular distribution in the moving system conveniently parametrized in the form $(1+b/a\cos^2\theta)/(1+b/3a)$.

Procedures for the analysis of the present data are described in the Appendix in detail as they differ somewhat from those in common use.[33,34] The systems are underdetermined, as unique values of the four parameters $v_{||}$, $v_\perp$, V, and b/a cannot, in general, be inferred from the three measured quantities. Rather, the data serve to establish correlations between and limits on the parameters. A typical example is given in the Appendix. It shows that the strongest correlation is between b/a and $v_\perp$. Depending on their values, fragment emission observed at 90° (in *PW*) may either be enhanced or depressed compared to that expected for isotropic emission in a forward moving system ($v_{||}$ and V only). Listed in Table III are values of b/a deduced from the present experiment assuming $v_\perp=0$. The values for incident protons and alpha particles scatter about and average close to zero, consistent with isotropic emission. On the other hand, those for incident ^{12}C ions at both energies are consistently negative. This is some evidence for enhanced sideward emission, either a negative anisotropy ($b/a<0$) in the ablation step or, what has the same effect, a nonzero value of $v_\perp$ (a sideward directed recoil from the abrasion step). While the present results are suggestive, more detailed experiments on fragment angular distributions from thin targets are necessary to draw firmer conclusions. In the sections which follow we focus on those quantities which are determined better in experiments of the present type.

Values of V and $\beta_{||}$ ($=v_{||}/c$) are plotted in Fig. 1 as a function of projectile rapidity Y. This is a convenient velocity related variable

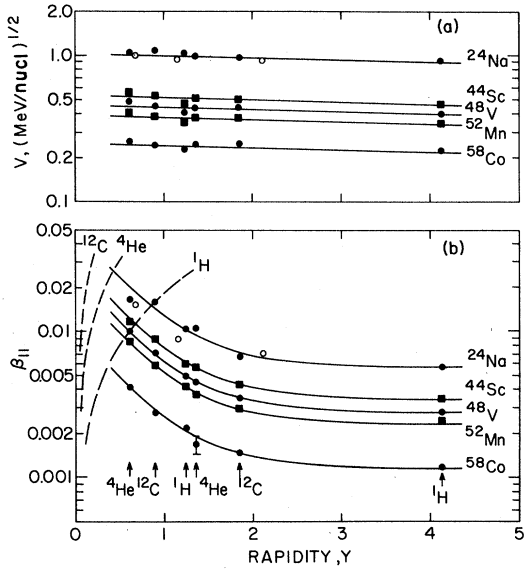

FIG. 1. Dependence of V [part (a)] and $\beta_{||}$ [part (b)] on projectile rapidity. Filled points are from the present work, those open are from Ref. 25. In each section of the figure the curves have the same shape but are vertically adjusted to fit the data for each isotope. The dashed curves in (b) show the dependence expected if a ^{1}H, ^{4}He, or ^{12}C projectile were captured by the Cu target. Projectile types for each group of points are indicated with arrows above the abscissa scale.

TABLE IV. Comparison of different procedures for the analysis of ^{24}Na production from Cu by 4.8-GeV ^{12}C ions.

Input	Range curve	V (MeV/nucleon)$^{1/2}$	$v_{\|\|}$ (MeV/nucleon)$^{1/2}$	Notes
FW,BW	$k(T/A)^{N/2}$	1.037±0.006	0.474±0.003	Ref. 24
FW,BW	$k(T/A)^{N/2}$	1.041±0.008	0.474±0.005	this work
FW,BW	polynomial	1.025±0.007	0.481±0.005	this work
FW,BW	$k(T/A)^{N/2}$	0.971±	0.483±	Ref. 34[a]
FW,BW,PW	polynomial	1.061±0.038	0.487±0.032	this work

[a]The program used did not have provision for error analysis.

($Y=\tanh^{-1}\beta=0.5\ \ln\ [(1+\beta)/(1-\beta)]$). Filled points are from the present experiment.[35] Open circles for ^{24}Na at Y values of 0.68, 1.16, and 2.12 were obtained from the data of Crespo *et al.*[25] for 0.88-GeV ^{4}He, 0.70-GeV ^{1}H, and 3-GeV ^{1}H, respectively, incident on Cu. Errors on the values of V arising from errors on the measured *FW*, *BW*, and *PW* are comparable to the size of the points in Fig. 1. Those on $\beta_{||}$ are somewhat larger, the largest being indicated on the point for ^{58}Co formed by ^{4}He ions at $Y=1.36$. We note that assumptions implicit in the analysis can introduce additional uncertainties beyond the purely statistical ones (see Table IV and Fig. 7). Because the same procedures were used throughout this work, Fig. 1 should give an overall picture from which the major trends of the kinematics of target fragmentation can be inferred.

An important feature of Fig. 1 is the monotonic dependence of both the abrasion step parameter $\beta_{||}$ and the ablation step parameter V on the mass of the observed product. Focusing on a particular product is tantamount, on the average, to selecting a subset from the wide range of excitations which occur in target fragmentation. In the study of 25-GeV ^{12}C and 28-GeV ^{1}H interactions,[24] both the variation with target-product mass difference and the absolute values of V were shown to agree with those predicted by a semiempirical model for deep-spallation reactions.[36] The present results [Fig. 1(a)] extend the range of that work and indicate that V is remarkably independent of the nature of the projectile (its mass or rapidity). There is more extensive ablation associated with the lighter products as expected. The straight lines in Fig. 1(a) suggest a small (17%) decrease in going from the lowest to highest rapidities, an effect not much larger than those which may be due to systematic errors in the analysis procedures. The overall picture of independence of the decay (ablation) mode from the formation mode suggests the validity of the factorization hypothesis in a similar way to that observed in cross section studies. In that case, single particle inclusive cross sections were found to depend on target-product mass difference but depended on projectile type only via the total cross section as a scaling factor.

Returning now to the first step of the reactions, values of $\beta_{||}$ [Fig. 1(b)] show, in addition to the dependence on final fragment mass, a much greater dependence on projectile rapidity than was seen for V. The solid lines in this figure have the same shape[37] but are vertically displaced for optimum fits to points for the different isotopes. They show the asymptotic behavior predicted by the limiting fragmentation hypothesis and, to the extent that points for different projectiles fall on a common curve for a given isotope, support the idea of factorization. In this case the projectile rapidity (or some other velocity related variable) and the final product mass are the important variables in determining momentum transfer in the abrasion phase of a target fragmentation reaction.

The general shape of the curves in Fig. 1(b) is similar to those observed for proton induced reactions such as ^{27}Al($p,3pn$)^{24}Na and ^{197}Au(p,x)^{149}Tb which have been studied over a wide range of energies.[38,39] The low values of $\beta_{||}$ and the inverse correlation between $\beta_{||}$ and Y indicate only partial momentum transfer between projectile and target in the initial step of the reaction. Shown by the three dashed curves in Fig. 1(b) are the values of $\beta_{||}$ appropriate for complete fusion between target and projectile. Except for products well removed from the target and at the lowest Y values, the present results are not consistent with the capture of even a single nucleon from the projectiles. We do anticipate that at some point there will be a transition between the solid and dashed curves. For the simple reaction, ^{24}Na production from Al,

Poskanzer's analysis[40] suggests that it occurs at $Y=0.36$ for ^{1}H and at 0.18 for ^{4}He projectiles. It will be of considerable interest to explore this region in detail for reactions of the type studied in the present work in order to connect complete-fusion and deeply inelastic interactions on the low side with the typical high-energy behavior which occurs for $Y \gtrsim 0.5$.

Values of $\tilde{\beta}_{||}$ for ^{48}V as a representative target fragment are plotted as a function of projectile kinetic energy in Fig. 2(a). The solid curves were obtained from the single curve for this isotope in Fig. 1 by the appropriate transformations from Y to T. With this choice of abscissa, it is apparent that deviations of $\beta_{||}$ from the limiting fragmentation value persist to progressively higher energies as projectile mass increases. The dashed curve in Fig. 2(a) is a prediction for ^{86}Kr, an ion which should be available in useful intensities from the upgraded LBL Bevalac. In this case, deviations of a factor of 2 are expected at kinetic energies of several tens of GeV.

The approach of the target fragment yield distribution to its limiting shape is shown in Fig. 2(b). This figure, taken from Ref. 16, is evidence both for factorization (because points for different projectiles fall on the same curve) and for limiting fragmentation (because of the energy independence

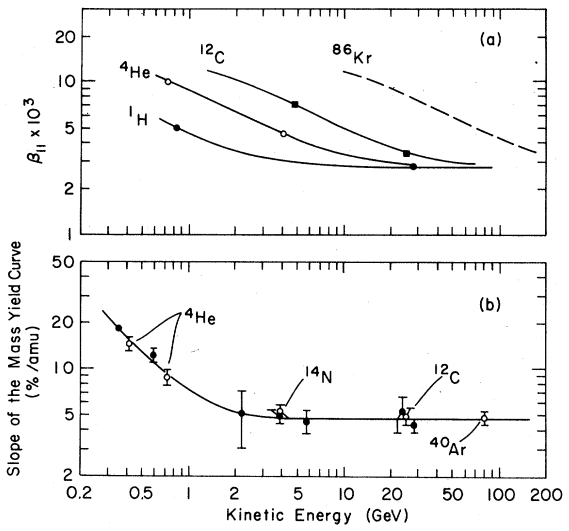

FIG. 2. Dependence of $\beta_{||}$ for ^{48}V formation [part (a)] and the slope of the mass yield curve [part (b)] for copper fragmentation on projectile kinetic energy. Points in (a) are from the present experiment. The curves were calculated from the curve for ^{48}V shown in Fig. 1(b). They are identified as to the appropriate projectile. (b) is taken from Ref. 16, which cites sources and details.

of the slope at kinetic energies above ~ 3 GeV). The importance of the comparison between Figs. 2(a) and 2(b) is that the yield distribution reaches its asymptotic limit at an appreciably lower energy than does the momentum transfer (as measured by $\beta_{||}$ values) in the initial steps of the target fragmentation process. While projectile kinetic energy may appear to be a good scaling variable for one fragment property, it may not be appropriate for another. We will show in the section which follows that this behavior can be understood in terms of simple models for the fragmentation process.

IV. MODELS FOR MOMENTUM TRANSFER

The above discussion of momentum transfer has emphasized the qualitative ideas of factorization and limiting fragmentation. A number of simple models have been proposed to treat quantitatively peripheral reactions involving small energy and momentum transfers from the bombarding particle. These all assume a two-step mechanism and treat the result of the abrasion step as a quasi-two-body system. Although differing in details of the initial interaction, they all predict the same functional form

$$\beta q_{||} = \Delta E_T [1 + k(1-\beta^2)^{1/2}] \tag{1}$$

for the dependence of longitudinal momentum transfer $q_{||}$ on the projectile's velocity β. Equation (1) is consistent with the limiting fragmentation hypothesis in that $q_{||}$ approaches the constant ΔE_T as β approaches unity and with factorization as well, if ΔE_T and k are independent of projectile. These models identify ΔE_T with the energy transferred to the prefragment. Strictly speaking, ΔE_T includes the excitation E^* of the prefragment which is subsequently dissipated in the ablation step, binding energy needed to remove nucleons (if any) from the target in the abrasion step, and kinetic energy of the recoiling prefragment. However, E^* is the major contributor for most reactions. Details of the assumed mechanism are contained in the dimensionless constant k which determines how rapidly the reduced momentum transfer $\beta q_{||}$ rises above its limiting value as the projectile velocity decreases. The experimental observation [Fig. 1(b)] that momentum transfer is a universal function of projectile rapidity requires that k be independent of projectile mass. We will return to k after first discussing the model independent quantity ΔE_T.

Values of ΔE_T for products studied in the present work are plotted in Fig. 3 as a function of mass number difference ΔA between target and product. These were obtained from the asymptotic values of $\beta_{||}$ from Fig. 1(b) with the assumption that the prefragment had $A=63$. Their uncertainties are estimated to be the order of $\pm 10\%$. Figure 3 shows the expected strong correlation between the length of the ablation cascade (as measured by ΔA) and the energy deposited in the abrasion step. This may be quantified in terms of the energies needed to reach the observed products.[41] The uppermost curve (nearly a straight line) in Fig. 3 labeled $(n+p)$ traces the minimum energies required to form the observed products by emission of individual nucleons. As expected, points for ^{58}Co to ^{44}Sc^{m} fall somewhat above this curve, the difference reflecting the kinetic energy of the emitted nucleons and nuclear recoil. For the lighter products, particularly ^{24}Na, there is essentially no excess, suggesting some heavier aggregates are emitted. The lower curve, that labeled $(n+p+\alpha)$ in Fig. 3, is that for product formation with the emission of the largest number of α particles. The general trend of the present data suggests some emission of nucleon aggregates during the longer ablation cascades, consistent with a semiempirical analysis of deep spallation reactions.[36]

As noted above, details of the physics of the various models are reflected in the constant k of Eq. (1). An early treatment of proton induced reactions, the single fast nucleon (SFN) model,[42]

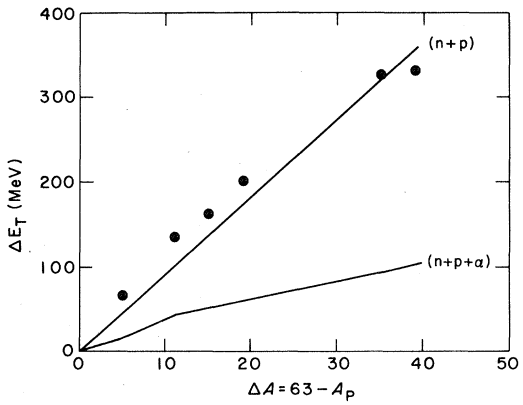

FIG. 3. Dependence of ΔE_T, the constant which determines the asymptotic limiting-momentum transfer, on mass number difference between the target and observed product. Points are from the present work. The curve labeled $(n+p)$ indicates energy required for forming the product by emission of individual nucleons. The lower curve labeled $(n+p+\alpha)$ is that for maximum emission of alpha particles.

assumed that the projectile was neither deflected nor excited in its initial interaction. Such a model predicts $k=0$ and a very weak (β^{-1}) dependence of $q_{||}$ on projectile velocity.

A less restrictive model, which has been applied extensively to proton induced reactions, has been proposed by Turkevich.[43] This assumes an elastic, grazing collision between the projectile and a target nucleon, in which the low-energy recoil nucleon is captured by the target and contributes excitation and momentum to the prefragment. For incident protons this model predicts $k=1$, or in the more general case, $k=1/m_p$, where m_p is the projectile mass. (In this and the following discussion, masses are expressed in units of the nucleon mass.)

In the collective tube model (CTM), the projectile is assumed to interact collectively with Δm_T of the nucleons in the target.[44] As applied to target fragmentation reactions,[45] this model leads to an equation of the form of Eq. (1) with $k=\Delta m_T/m_p$. For two well-studied, proton-induced reactions, k was found to be 0.9 ± 0.2 for ^{24}Na production from ^{27}Al, and 3.1 ± 0.4 for ^{149}Tb production from ^{197}Au. Winsberg[46] has extended this analysis to a variety of other reactions and had deduced values of k ranging from near zero to 12.7. The larger values were found to be associated with large mass losses from heavy element targets.

Several models have been developed specifically for heavy ion projectiles. The friction treatment of Abul-Magd *et al.*[47] considers the abrasion step in terms of a multiple independent collision model (MICM), each step of which involves transfer of a small momentum to an individual target nucleon. The "friction" loss as the struck nucleon climbs out of the target potential well heats the nucleus (giving rise to ΔE_T) and transfers momentum $q_{||}$ to it. The kinematics of a single step leads to $k=1$. If the velocity of the exciting projectile remains nearly constant, then the result of a series of steps will have the same form as Eq. (1) with values of ΔE_T and $q_{||}$ appropriate for the overall process.

The dual nova model of Masuda and Uchiyama[48] assumes diffractive excitation of both beam and target nuclei, with no exchange or loss of mass or charge, to produce target and beam novas with excitation energies ΔE_t and ΔE_B, respectively. For this model, $k=\Delta E_B/\Delta E_T$. As expected, when the beam particle is not excited $(\Delta E_B=0)$ the kinematics become identical with those of the SFN model.

The dimensionless quantity $\beta q_{||}/\Delta E_T$ is plotted vs $(1-\beta^2)^{1/2}$ in Fig. 4. This choice of ordinate serves to remove the strong dependence of $q_{||}$ on

product. Equation (1) predicts a linear relationship between these variables, rising with slope k from a unit intercept. The points in Fig. 4 exhibit this general trend. Individual points for ^{58}Co and ^{24}Na have been connected by short- and long-dashed lines, respectively, to examine any dependence of k on product. This generally appears to be small. The solid line in Fig. 4 is that for $k=1$. The points scatter about it with an rms deviation of 9%. Fitting all the data with k as a free parameter gave a value of 1.11 ± 0.13 with no significant improvement in the quality of the fit. Least squares analyses for individual isotopes gave k values ranging from 0.9 to 1.3 with relatively large errors of ±0.3. Winsberg[46] has deduced that $k=1.3\pm0.3$ for ^{24}Na production from Cu by high-energy protons, consistent with the present result for a wider range of projectiles.

Figure 4 is clearly at variance with the $k=0$ predicted by the SFN model and the special case of the dual nova model in which there is no beam excitation. In the general case, $k=\Delta E_B/\Delta E_T$. We have evidence that ΔE_T is relatively independent of projectile type from the near independence of V on projectile mass or energy [Fig. 1(a)]. Constancy of k then implies a commensurate independence of ΔE_B. Since the density of states available is so different for ^{1}H, ^{4}He, and ^{12}C projectiles, this would appear to require an unlikely accident.

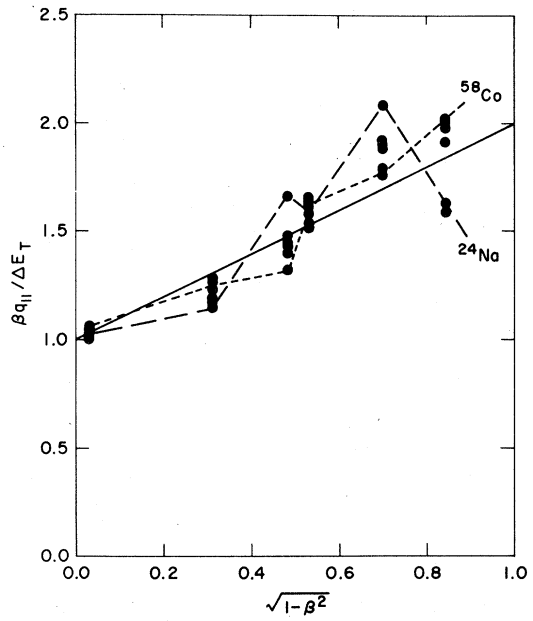

FIG. 4. Analysis of momentum transfers in the fragmentation of Cu by various projectiles in terms of an equation [Eq. (1)] based on general kinetical considerations. The points are from the present experiment. The solid line is that predicted for $k=1$. The dotted and dashed lines connect individual points for ^{24}Na and ^{58}Co, respectively.

The reciprocal dependence of k on m_p predicted by the original forms of the Turkevich model and the CTM also is not consistent with the data. For example, if $k=1=\Delta m_T/m_p$, then for $m_p=12$, Δm_T would equal 12, an absurd result for the formation of ^{58}Co from Cu. Such a failure might have been expected when the projectile is a complex nucleus. In a peripheral collision, only some fraction Δm_p of its mass may be effective and k would become $1/\Delta m_p$ or $\Delta m_T/\Delta m_p$ for the Turkevich and CTM, respectively. In the absence of any collective effects, both models reduce to $k=1$, the same value predicted by MICM of the friction type. It has been noted[46] that significant collective effects ($k>>1$) appear to be confined to targets appreciably heavier than copper.

The general consistency of the data on copper fragmentation with the hypotheses of limiting fragmentation and factorization and with the simple kinematical model suggests that Eq. (1) might be a useful framework for examining data from other target systems. While an extensive review is

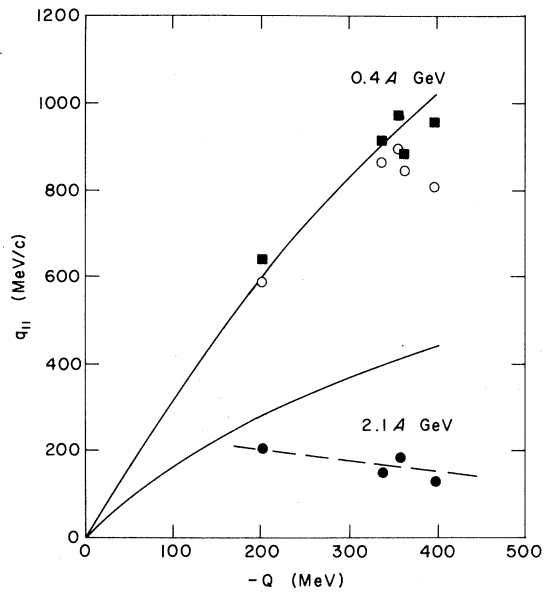

FIG. 5. Comparison of momentum transfers to products of the fragmentation of gold with corresponding products from copper. The upper and lower solid curves are determined by the present results for 4.8- and 25-GeV ^{12}C, respectively, incident on copper. The points are for gold targets and 25-GeV ^{12}C (●), 4.8-GeV ^{12}C (○), or 7.6-GeV ^{20}Ne (■) projectiles from Refs. 26 and 49. The dashed curve shows the general trend of the highest energy results.

beyond the scope of the present paper, some comparisons will serve to point up the similarities and differences between copper and heavier targets.

Momentum transfers in the fragmentation of gold targets by heavy ions[26,29] are compared in Fig. 5 with those observed in the present work. In this comparison, the assumption has been made that reactions requiring the same energy deposition ΔE_T will have the same $q_{||}$ if k does not depend on target. Furthermore, $-Q$, the energy needed to form the product by nucleon emission, has been used as an approximation to ΔE_T. A strong correlation between ΔE_T and $-Q$ has been shown in Fig. 3. For targets over a narrower mass range, comparison at constant ΔA might be equally satisfactory.

Data for 4.8-GeV ^{12}C ions incident on gold (open circles) and for 7.6-GeV ^{20}Ne (filled squares) fall reasonably close to the curve labeled 0.4A GeV in Fig. 5 which is defined by the present experiments with 4.8-GeV ^{12}C. Kaufman *et al.*[49] have noted the near equality of the momentum transfers for these ^{12}C and ^{20}Ne ions which have nearly the same velocity. This and the agreement with the copper results are consistent with the $k=1$ form of Eq. (1).

Major differences appear for the higher velocity projectiles. Observed momentum transfers for 25-GeV ^{12}C ions incident on gold[26] (filled circles in Fig. 5) fall well below those observed when the same projectile is incident on Cu (the lower solid curve). However, the trend of the gold data as shown by the dashed line suggests an approach to the Cu curve if data for products nearer the target were available.

Longitudinal momenta transferred to fragments with $A\sim149$ by the interactions of energetic protons and heavy ions with gold are compared in Fig. 6 in a form suggested by Eq. (1). Crosses are results for ^{149}Tb production by protons.[50] The high velocity portion of these data $[(1-\beta^2)^{1/2}<0.4]$ has been taken as evidence for collective effects ($k=3.1$ as shown by the dashed line) in this target system. However, bending of the solid curve, which indicates the trend of the proton data, shows that Eq. (1), with constant values of both ΔE_T and k, is not valid, even for a single projectile, over the whole range covered here.

Points for heavy projectiles in Fig. 6 are averages of data[26,29] for ^{149}Gd, ^{146}Gd, and ^{145}Eu to reduce scatter. Momentum transfers for the lower energy ions (4.8-GeV ^{12}C and 7.6-GeV ^{20}Ne) are consistent with a reasonable extrapolation of the proton data

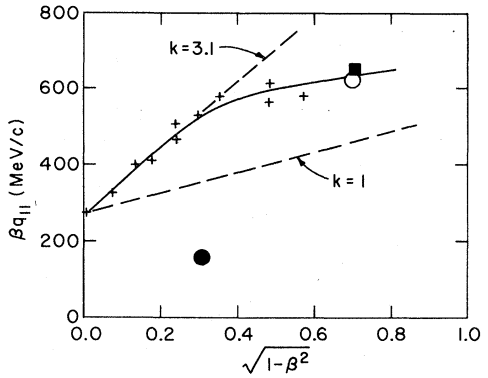

FIG. 6. Comparison of reduced momenta $\beta q_{||}$ for fragmentation reactions in gold leading to products with $A\sim149$. Symbols are: + for protons of several energies; ○ for 4.8-GeV ^{12}C; ● for 25-GeV ^{12}C; and ■ for 7.6-GeV ^{20}Ne. The solid line traces the general trend of the proton data. Dashed lines labeled $k=3.1$ and $k=1$ indicate the dependence predicted by the simple model [Eq. (1)] with and without collective effects.

as would be expected if factorization were valid. However, the point for 25-GeV ^{12}C falls well below the curve for protons at any velocity. Kaufman *et al.*[49] have suggested that this more rapid decrease might be due to greater collectivity for the heavy ions. The apparently negative asymptotic limiting value of $q_{||}$ for the heavy projectiles is a serious problem for such an interpretation in terms of Eq. (1). It is interesting to note that the fireball model[5] could not account for spectra of energetic particles from the highly excited participant region when the bombarding particle was a 2.1A-GeV ^{20}Ne but did give satisfactory fits at 0.25A and 0.4A GeV.

Failure of any simple model to account for complex reactions induced by high-energy heavy ions in heavy element targets might have been anticipated from results when energetic protons are the bombarding particle. Abnormally low momentum transfers have been reported for a variety of products in these proton induced reactions. Thick-target, thick-catcher studies[51] have indicated essentially zero $q_{||}$ for products such as ^{48}V from gold at 28 and 300 GeV, despite the fact that excitation functions show that large deposition energies are necessary for their formation. A recent analysis[52] of ^{128}Ba production from U in terms of Eq. (1) has given a surprisingly low value for ΔE_T, 67 MeV, for this reaction which involves loss of 110 nucleons from the target, and a high value for k, 27. Measurements of angular distributions[53–56] have shown, in addition to the development of sideward peaking,[53] that many fragments from both U and

Au are emitted preferentially into the backward hemisphere in the laboratory system.[54–56]

Perhaps more importantly, some experimental data indicate a failure of the two step picture which underlies the models and the analysis of the experimental results. For proton energies in the 2–6 GeV region, intensities of fragments such as ^{24}Na in the forward direction are too large to be consistent with the observed values of $q_{||}$.[57,58] Even more surprising is the observation that the direction of the breakdown of the two step model reverses at very high energies. At 400 GeV, the observed excess of Sc fragments in the backward direction is not the consequence of negative $q_{||}$.[59]

V. SUMMARY

Thick-target, thick-catcher studies of the interaction of ^{1}H, ^{4}He, and ^{12}C with Cu have been analyzed to give mean kinetic properties of the abrasion and ablation steps of these fragmentation reactions. Longitudinal momentum transfers in the abrasion stage are shown to be a strong function of the mass of the final product and to depend on the rapidity (or other velocity related variable) of the projectile. These data and those existing for fragment cross sections are discussed in terms of the hypotheses of limiting fragmentation and factorization. It is shown that the apparently conflicting dependences of yield pattern on projectile kinetic energy and of the momenta on projectile velocity can be reconciled in terms of a simple kinematic model in which the initial interaction is either a single collision between a projectile nucleon and a target nucleon, or a series of such collisions each involving small transfers of energy and momenta. Extension of this picture to heavy target elements is only partially successful. Large deviations are observed for high-energy (2.1A GeV) heavy ions for products 30 or more nucleons removed from the target, although general agreement is seen at 0.4A GeV for products as much as 50 nucleons removed. The behavior of the more energetic heavy ions represents a continuation of trends observed for high-energy protons which involve the onset of reaction mechanisms which are not well understood.[60]

This research was performed under contract with the U.S. Department of Energy.

APPENDIX: ANALYSIS OF THICK-TARGET RECOIL DATA

Various procedures[33,34] have been developed for deriving the two-step model parameters $v_{||}$, $v_{\perp}$, V, and b/a from the values of FW, BW, and PW measured in thick-target, thick-catcher recoil experiments. In general, these entail truncation of series expansions in the quantities $n_{||}=v_{||}/V$ and $\eta_{\perp}=v_{\perp}/V$ which may not be valid if $\eta_{||}$ or $n_{\perp}$ are large. The procedure described below does not use such expansions and permits examination of correlations between parameters as well as effects of some of the assumptions in other methods of data analyses on them.

For the analysis of the present data, range-energy curves for ^{44}Sc^{m}, ^{48}V, ^{52}Mn, and ^{58}Co in Cu were obtained as polynomial approximations to log-log plots of the values tabulated by Northcliffe and Schilling.[61] For ^{24}Na and ^{28}Mg, more recent data from Winsberg[62] were used. We have combined these range-energy curves with a numerical integration procedure to calculate FW, BW, and PW from trial values of the parameters V, $v_{||}$, $v_{\perp}$, and b/a. This calculation was incorporated into a nonlinear least-squares program which refined the parameters for optimum agreement with experimental values. While the system is underdetermined in that, at most, three parameters can be determined from the three input data (FW, BW, and PW), we are able, by fixing values of the fourth parameter, to explore sets of the parameters which are consistent with the experimental data and to estimate how sensitive the various derived quantities are to assumptions concerning the others.

The above procedure differs from those in common use[33,34] in that it does not assume a power law dependence of range on energy ($R=k(T/A)^{N/2}$), or the validity of series expansions if $v_{\perp}$ and b/a are nonzero. It still, however, assumes unique values of parameters rather than distributions of them. The effects of some of these changes are explored in Table III for the production of ^{24}Na by 4.8-GeV ^{12}C ions. Line 1 gives values of V and $v_{||}$ obtained from FW and BW using the conventional procedures which were used in the previous work from this laboratory.[24,28] Substitution of the numerical integration (line 2) for the series expansions causes negligible changes as expected since b/a and $v_{\perp}$ have been forced to zero. Introduction of the polynomial range curve (line 3) also results in small changes. Line 4 shows results of an analysis using a procedure due to Winsberg[34] which includes a distribution of V but none for $v_{||}$. The derived value of V (average in this case) is reduced by $\sim$5%, but $v_{||}$ remains nearly the same.

The last line in Table IV shows the results of

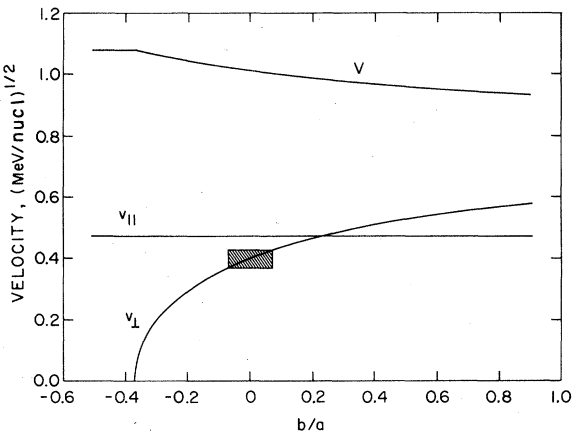

FIG. 7. Dependence of V, $v_{||}$, and $v_\perp$ on values of b/a assumed in analyzing the experimental data for ^{24}Na production from Cu by 4.8-GeV ^{12}C ions. The cross hatched rectangle is a measure of the effects of experimental errors in the analysis of the $v_\perp$-(b/a) correlation. It does not indicate this value is more to be preferred than any other along the curve labeled $v_\perp$.

forcing all three measured quantities, *FW*, *BW*, and *PW*, to fit two parameters. Higher values of both V and $v_{||}$ are obtained and larger errors indicate that the quality of the fit is ~ 7 times poorer than would have been expected from the errors on *FW*, *BW*, and *PW*. The observed value of *PW* is larger than that expected for isotropic emission from a forward moving system, suggesting that b/a or $v_\perp$ are nonzero. This is explored in more detail in Fig. 7. Here b/a plays the role of the independent variable and V, $v_{||}$, and $v_\perp$ are adjusted by the least-squares program for optimum fits to the input data. To the left of the intersection of the $v_\perp$ curve with the abscissa at $b/a = -0.37$, values of *FW*, *BW*, and *PW* cannot be fit exactly by the model. A nonphysical $v_\perp{}^2 < 0$ would be required in this region.

To the right of $b/a = -0.37$, $v_\perp$ and b/a play competing roles with the curve denoted $v_\perp$ in Fig. 1 tracing the locus of pairs of values consistent with the data. It is apparent from Fig. 1 that the present sort of experiment cannot, over a wide range of values, resolve whether the excess emission observed in the P catchers is due to a first stage directed motion ($v_\perp$) or a second step anisotropy (b/a). However, the value of $v_{||}$ depends only slightly on either assumption while that of V appears anticorrelated with $v_\perp$, decreasing by 13% as $v_\perp$ increases from 0 to 0.58, in the region illustrated in Fig. 6.

The position of the intercept in Fig. 6 is useful in characterizing preferred directions of emission. In the illustrative case (negative intercept), excess recoils are observed in the P catchers. If the intercept were at $b/a = 0$, the emission could not be ruled out as occurring isotropically in a forward moving system. On the other hand, an intercept at $b/a > 0$ would imply a preference for forward-backward emission. Results from the present experiments are given in Table III.

[1]M. G. White, M. Isaila, K. Prelec, and H. L. Allen, Science 174, 1121 (1971).
[2]H. A. Grunder, W. D. Hartsough, and E. J. Lofgren, Science 174, 1128 (1971).
[3]For a recent review of this topic, see A. S. Goldhaber and H. H. Heckman, Annu. Rev. Nucl. Part. Sci. 28, 161 (1978).
[4]J. D. Bowman, W. J. Swiatecki, and C. F. Tsang, Lawrence Berkeley Laboratory Report No. LBL-2908, 1973 (unpublished).
[5]G. D. Westfall, J. Gosset, P. J. Johansen, A. M. Poskanzer, W. G. Meyer, H. H. Gutbrod, A. Sandoval, and R. Stock, Phys. Rev. Lett. 37, 1202 (1976).
[6]W. D. Myers, Nucl. Phys. A296, 177 (1978).
[7]J. Hufner and J. Knoll, Nucl. Phys. A290, 460 (1977).
[8]H. H. Heckman, H. J. Crawford, D. E. Greiner, P. J. Lindstrom, and L. W. Wilson, Phys. Rev. C 17, 1651 (1978).
[9]A. Sandoval, H. H. Gutbrod, W. G. Meyer, R. Stock, Ch. Lukner, A. M. Poskanzer, J. Gosset, J.-C. Jourdain, C. H. King, G. King, Nguyen Van Sen, G. D. Westfall, and K. L. Wolf, Phys. Rev. C 21, 1321 (1980).
[10]See the review by H. Boggild and T. Ferbel, Annu. Rev. Nucl. Sci. 24, 451 (1974).
[11]D. E. Greiner, P. J. Lindstrom, H. H. Heckman, B. Cork, and F. S. Bieser, Phys. Rev. Lett. 35, 152 (1975).
[12]P. J. Lindstrom, D. E. Greiner, H. H. Heckman, B. Cork, and F. S. Bieser, Lawrence Berkeley Laboratory Report No. LBL 3650, 1975 (unpublished).
[13]G. D. Westfall, Lance W. Wilson, P. J. Lindstrom, H. J. Crawford, D. E. Greiner, and H. H. Heckman, Phys. Rev. C 19, 1309 (1979).
[14]J. B. Cumming, P. E. Haustein, R. W. Stoenner, L. Mausner, and R. A. Naumann, Phys. Rev. C 10, 739 (1974).
[15]J. B. Cumming, R. W. Stoenner, and P. E. Haustein, Phys. Rev. C 14, 1554 (1976).
[16]J. B. Cumming, P. E. Haustein, T. J. Ruth, and G. J. Virtes, Phys. Rev. C 17, 1632 (1978).
[17]C. R. Rudy and N. T. Porile, Phys. Lett. 59B, 240

(1975).
[18]N. T. Porile, G. D. Cole, and C. R. Rudy, Phys. Rev. C 19, 2288 (1979).
[19]D. J. Morrissey, W. Loveland, and G. T. Seaborg, Z. Phys. A 289, 123 (1978).
[20]D. J. Morrissey, W. Loveland, M. de Saint Simon, and G. T. Seaborg, Phys. Rev. C 21, 1783 (1980).
[21]W. Loveland, R. J. Otto, D. J. Morrissey, and G. T. Seaborg, Phys. Lett. 69B, 284 (1977).
[22]S. B. Kaufman, E. P. Steinberg, D. Wilkins, and D. J. Henderson, Phys. Rev. C 22, 1897 (1980).
[23]W. Loveland, R. J. Otto, D. J. Morrissey, and G. T. Seaborg, Phys. Rev. Lett. 39, 320 (1977).
[24]J. B. Cumming, P. E. Haustein, and H.-C. Hseuh, Phys. Rev. C 18, 1372 (1978).
[25]V. P. Crespo, J. M. Alexander, and E. K. Hyde, Phys. Rev. 131, 1765 (1963).
[26]S. B. Kaufman, E. P. Steinberg, and B. D. Wilkins, Phys. Rev. Lett. 41, 1359 (1978).
[27]W. Loveland, D. J. Morrissey, K. Aleklett, G. T. Seaborg, S. B. Kaufman, E. P. Steinberg, B. D. Wilkins, J. B. Cumming, P. E. Haustein, and H. C. Hseuh, Phys. Rev. C 22, 253 (1981).
[28]P. E. Haustein, J. B. Cumming, and H.-C. Hseuh, in Proceedings of The Symposium on Heavy Ion Physics from 10 to 200 MeV/amu, edited by J. Barrette and P. D. Bond, Brookhaven National Laboratory Report No. BNL-51115, 1979, p. 561.
[29]A. M. Poskanzer, J. B. Cumming, and R. Wolfgang, Phys. Rev. 129, 374 (1963).
[30]N. Sugarman, M. Campos, and K. Wielgoz, Phys. Rev. 101, 388 (1956).
[31]N. T. Porile and N. Sugarman, Phys. Rev. 107, 1410 (1957).
[32]N. Sugarman, H. Munzel, J. A. Panontin, K. Wielgoz, M. V. Ramaniah, G. Lange, and E. Lopez-Menchero, Phys. Rev. 143, 952 (1966).
[33]J. M. Alexander, in *Nuclear Chemistry,* edited by L. Yaffe (Academic, New York, 1968), Vol. I, p. 273; L. Winsberg and J. M. Alexander, *ibid.,* p. 340.
[34]L. Winsberg, Nucl. Instrum. Methods 150, 465 (1978).
[35]Results for ^{28}Mg have not been included in Fig. 1 to avoid overlap with those for ^{24}Na. They fell close to, but slightly below (on the average) those for ^{24}Na.
[36]V. P. Crespo, J. B. Cumming, and J. M. Alexander, Phys. Rev. C 2, 1777 (1970).
[37]The curves are the function $\beta_{\|}=\beta_{\|}^{\infty}(1+8.112e^{-1.848Y})$ with values of $\beta_{\|}^{\infty}$ adjusted to best fit data for each product.
[38]L. Winsberg, E. P. Steinberg, D. Henderson, and A. Chrapkowski, Phys. Rev. C 22, 2108 (1980), and earlier work cited therein.
[39]L. Winsberg, M. W. Weisfield, and D. Henderson, Phys. Rev. C 13, 279 (1976), and earlier work cited therein.
[40]A. M. Poskanzer, Phys. Rev. 129, 385 (1963).
[41]Binding energy differences were calculated from the mass tables of A. H. Wapstra and K. Bos, At. Data Nucl. Data Tables 19, 175 (1977).
[42]S. C. Fung and T. Perlman, Phys. Rev. 87, 622 (1952).
[43]A. Turkevich, quoted in Ref. 31.
[44]G. Berland, A. Dar, and G. Eilam, Phys. Rev. D 13, 161 (1976); Meng Ta-Chung, *ibid.* 15, 197 (1977).
[45]J. B. Cumming, Phys. Rev. Lett. 44, 17 (1980).
[46]L. Winsberg, Phys. Rev. C 22, 2123 (1980).
[47]A. Abul-Magd, J. Hufner, and B. Schurmann, Phys. Lett. 60B, 327 (1976).
[48]N. Masuda and F. Uchiyama, Phys. Rev. C 15, 1598 (1977).
[49]S. B. Kaufman, E. P. Steinberg, B. D. Wilkins, and D. J. Henderson, Phys. Rev. C 22, 1897 (1980).
[50]L. Winsberg, M. W. Weisfield, and D. Henderson, Phys. Rev. C 13, 279 (1976), and earlier work cited therein.
[51]S. B. Kaufman, E. P. Steinberg, and M. W. Weisfield, Phys. Rev. C 18, 1349 (1978).
[52]S. Pandian and N. T. Porile, Phys. Rev. C 23, 427 (1981).
[53]L. P. Remsberg and D. G. Perry, Phys. Rev. Lett. 35, 361 (1975).
[54]N. T. Porile, D. R. Fortney, S. Pandian, R. A. Johns, T. Kaiser, K. Wielgoz, T. S. K. Chang, N. Sugarman, J. A. Urbon, D. J. Henderson, S. B. Kaufman, and E. P. Steinberg, Phys. Rev. Lett. 43, 918 (1979).
[55]D. R. Fortney and N. T. Porile, Phys. Rev. C 21, 2511 (1980).
[56]R. L. Klobuchar, G. J. Virtes, and J. B. Cumming (unpublished).
[57]J. B. Cumming, R. J. Cross, J. Hudis, and A. M. Poskanzer, Phys. Rev. 134, B167 (1964).
[58]A. M. Poskanzer, G. W. Butler, and E. K. Hyde, Phys. Rev. C 3, 882 (1971).
[59]D. R. Fortney and N. T. Porile, Phys. Rev. C 22, 670 (1980).
[60]B. D. Wilkins, S. B. Kaufman, E. P. Steinberg, J. A. Urbon, and D. J. Henderson, Phys. Rev. Lett. 43, 1080 (1979).
[61]L. C. Northcliffe and R. F. Schilling, Nucl. Data A7, 233 (1970).
[62]L. Winsberg, At. Data Nucl. Data Tables 20, 389 (1977).